

CHEMISTRY

A EUROPEAN JOURNAL

Supporting Information

© Copyright Wiley-VCH Verlag GmbH & Co. KGaA, 69451 Weinheim, 2008

Understanding the Two-Step Spin Transition Phenomenon in Iron(II) 1-D Chain Materials

Suzanne M. Neville,^{*,[a]} Benjamin A. Leita,^[a] Gregory J. Halder,^[b, c] Cameron J.
Kepert,^[b] Boujemaa Moubaraki,^[a] Jean-François Létard^[d] and Keith S.
Murray.^{*,[a]}

*[a] School of Chemistry, Monash University, Building 23, Clayton, VIC 3800, Australia. Fax: (+)61
3 9905 4597*

[b] School of Chemistry, The University of Sydney, NSW 2006, Australia.

[c] Materials Science Division, Argonne National Laboratory, Argonne, Illinois, 60439, USA.

*[d] Laboratoire des Sciences Moléculaires, ICMCB (CNRS UPR 9048), Université Bordeaux I,
33608 Pessac, France.*

Contents.

S1. Magnetic Susceptibility Measurements

Figure S1. $c_M T$ versus temperature for $\text{Fe}(\text{NCS})_2(\text{bdpp})$, **2a**, over the range 4-300

K.

Figure S2. $c_M T$ versus temperature for $\text{Fe}(\text{NCSe})_2(\text{bdpp})$, **2b**, over the range 4-300 K with fast cooling.

S2. LIESST Measurements by Magnetic Susceptibility

Figure S3. Comparison of the $T(\text{LIESST})$ experimental and simulated (red curve) for **2b** obtained from the thermodynamic parameters deduced from the kinetics : $E_a = 165 \text{ cm}^{-1}$, $k_\infty = 0.14 \text{ s}^{-1}$ and $k_0 = 1.5 \cdot 10^{-4} \text{ s}^{-1}$

S3. Single Crystal X-ray Diffraction

Figure S4. ORTEP representation (50 % probability) of the crystal structure of **1** at 25 K highlighting the numbering scheme. The same scheme is used for **1**^{LS-LS}, **1**^{LS-HS} and **1**^{HS-HS}.

Figure S5. ORTEP representation (50 % probability) of the crystal structure of **2a** at 123 K highlighting the numbering scheme.

Figure S6. ORTEP representation (50 % probability) of the crystal structure of **2b** at 100 K highlighting the numbering scheme. The same scheme is used for **2b**^{LS}, **2b**^{LS/HS} and **2b**^{HS}.

S1. Magnetic Susceptibility Measurements

Magnetic susceptibility measurements were carried out for each of the materials **1**, **2a** and **2b** over the temperature range 4- 275 K in both the heating and cooling modes. The $c_M T$ versus temperature plots for **1** and **2b** are located in the main text of the manuscript. Described here are the magnetic susceptibility measurements for **2a** and extra measurements for **2b** not discussed in the text.

Magnetic susceptibility measurements on **2a** revealed a HS state for the iron(II) centres over all temperatures (Figure S1). The $c_M T$ values of *ca.* $3.5 \text{ cm}^3 \text{ K mol}^{-1}$ over the range 275 – 150 K are consistent with that expected for HS iron(II). Below 150 K there is a slight decrease in $c_M T$ values to a minimum of *ca.* $3.25 \text{ cm}^3 \text{ K mol}^{-1}$ likely reflecting a small impurity of **1** as crystalline samples of these materials are formed together and must be separated by hand. The bulk of the sample is **2a** thus it is not surprising that **1** would contain a small amount of **1**. In any case it is obvious that it remains HS over all temperatures. Lastly, the drop in $c_M T$ values below 10 K is commonly observed for iron(II) SCO species and is due to combination of weak antiferromagnetic coupling and zero field splitting.

Magnetic susceptibility measurements for the two-step SCO for **2b** are reported in the text (Figure 3). Initially, a gradual one-step SCO was observed which showed significant trapping of a HS species at low temperatures with or without quench-cooling (Figure S2). Firstly, the trapped HS species is due to torquing effects as when the sample was placed in Vaseline it was no longer observed. Additionally, when the sample was both cooled/heated at a slower rate, especially at low temperatures where longer equilibration times are often needed to avoid thermal trapping of HS species, this one-step behaviour was not observed only the reported two-step behaviour.

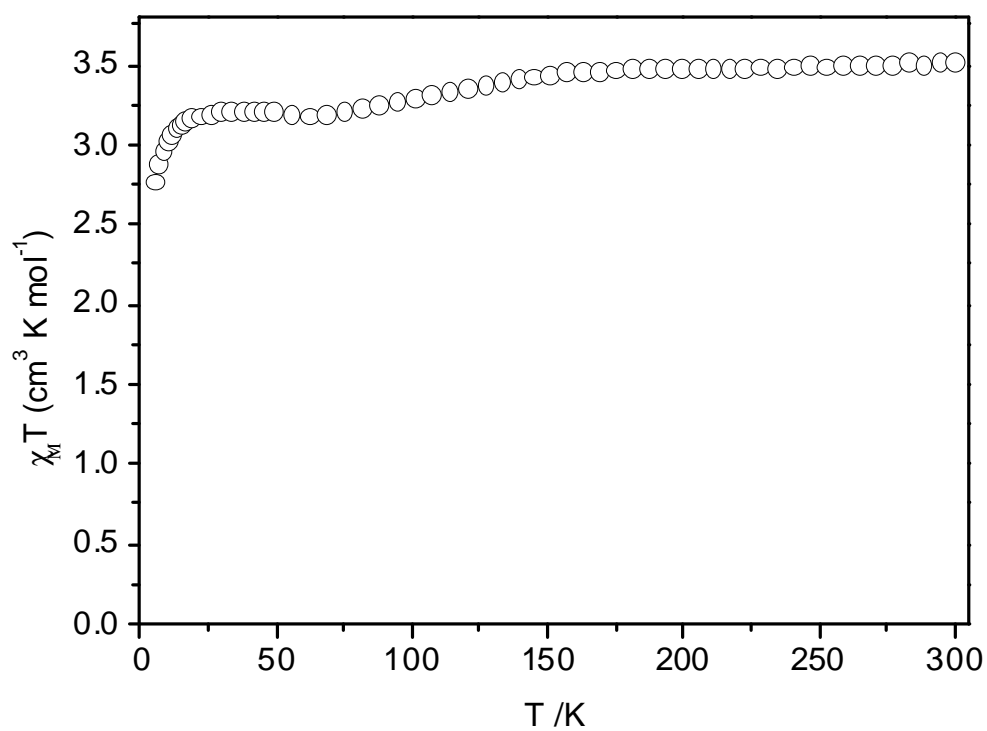


Figure S1. $c_M T$ versus temperature for $\text{Fe}(\text{NCS})_2(\text{bdpp})$, **2a**, over the range 4-300

K.

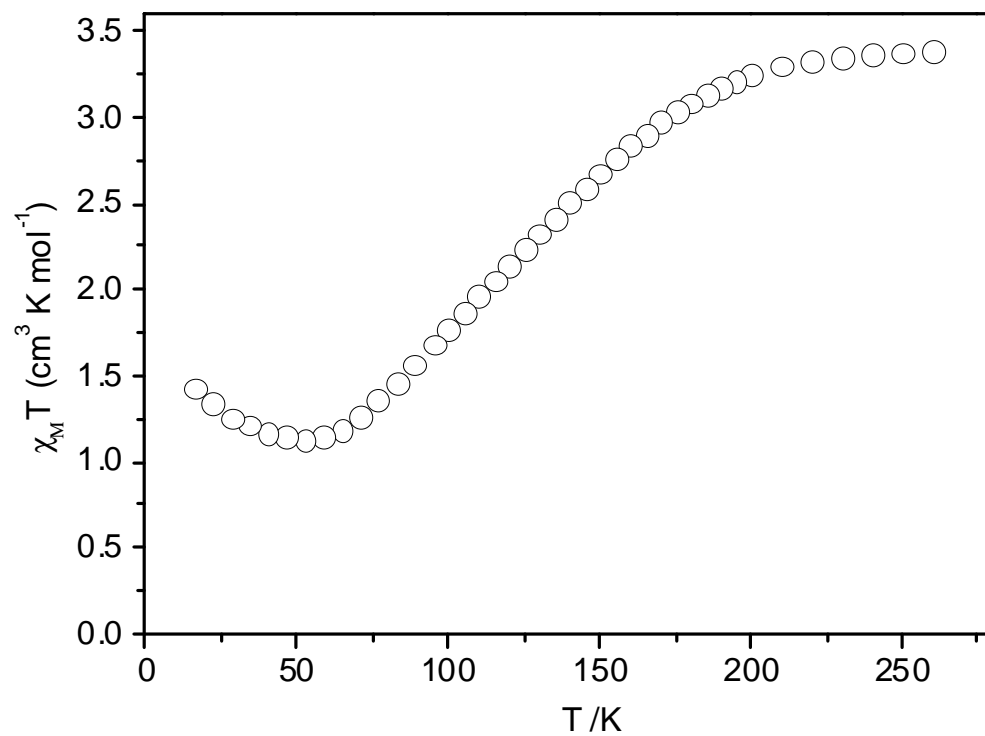


Figure S2. $c_M T$ versus temperature for $\text{Fe}(\text{NCSe})_2(\text{bdpp})$, **2b**, over the range 4-275

K.

S2. LIESST Measurements by Magnetic Susceptibility

The time-dependence of the relaxation of the metastable HS fraction of **2b** in the absence of irradiation was carried out. The relaxation kinetics were carried out at the following temperatures; 40, 46, 50 and 55 K. At all temperatures the plots were fitted to a stretched exponential behavior. The E_a value calculated using the straight line fit through the data points in the Arrhenius plot is 165 cm^{-1} . The stretched exponential shape of the relaxation curves and low the E_a value is consistent with low cooperativity in this system.

These parameters, together with $k_o = 1.5 \times 10^{-4} \text{ s}^{-1}$ (the overestimated limit of the tunneling rate constant), were also used to confirm the stretched exponential model and simulate the $T(\text{LIESST})$ experimental curve given in Figure 3; the best fit curve, is very good (Figure S3).

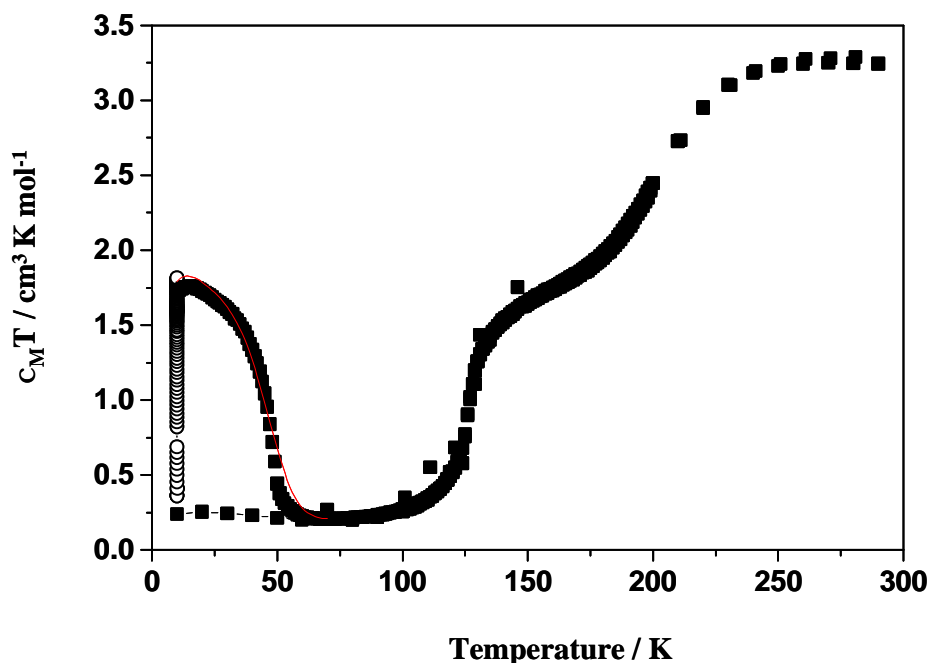


Figure S3. Comparison of the $T(\text{LIESST})$ experimental and simulated (red curve) for **2b** obtained from the thermodynamic parameters deduced from the kinetics : $E_a = 165 \text{ cm}^{-1}$, $k_\infty = 0.14 \text{ s}^{-1}$ and $k_0 = 1.5 \times 10^{-4} \text{ s}^{-1}$

S3. Single Crystal X-ray Diffraction

Single crystal diffraction for Fe(NCS)₂(bdpp) (**1** and **2a**) and Fe(NCSe)₂(bdpp) (**2b**) were carried out at various temperatures based on their individual magnetic susceptibility results. Polymorph **1** showed a two-step SCO. The appropriate temperatures for data collection where a plateau region was present were 25 K, 123 K and 250 K. Thus the structures of polymorph were obtained in the **1**^{LS-LS}, **1**^{LS-HS} and **1**^{HS-HS} states. Polymorph **2a** showed a HS state over all temperature so a standard structure was carried out at 123 K. The material **2b** showed a two-step SCO occurring at higher temperatures than **1**. The appropriate temperatures for data collection where a plateau region was present were 90 K, 150 K and 250 K. Thus the structures were obtained in the **2b**^{LS}, **2b**^{LS/HS} and **2b**^{HS} states.

The numbering scheme of the materials, i.e. **1**, **2a** and **2b** was chosen such that the isostructural materials **2a** and **2b** were group together rather than labeling the polymorphs **1** and **2a** jointly. Furthermore, the superscript of the materials **1** and **2b** at various temperatures refers to the spin state of the iron(II) centres and highlights that two crystallographically distinct metal sites were observed in **1** and one in **2b**.

Following are representative ORTEP diagrams of the structures **1**^{LS-LS} (Figure S4), **2a** (Figure S5) and **2b**^{LS} (Figure S6) with numbering schemes of all the atoms in the respective asymmetric units.

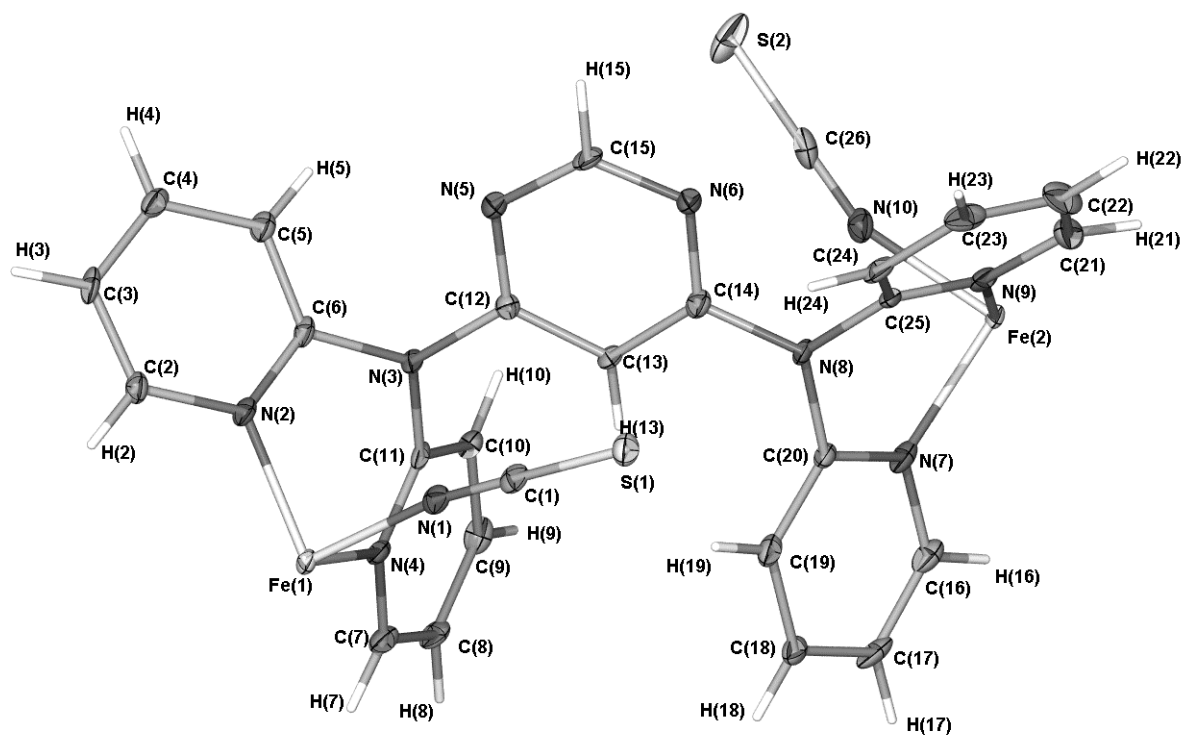


Figure S4. ORTEP representation (50 % probability) of the crystal structure of **1** at 25 K highlighting the numbering scheme. The same scheme is used for **1**^{LS-LS}, **1**^{LS-HS} and **1**^{HS-HS}.

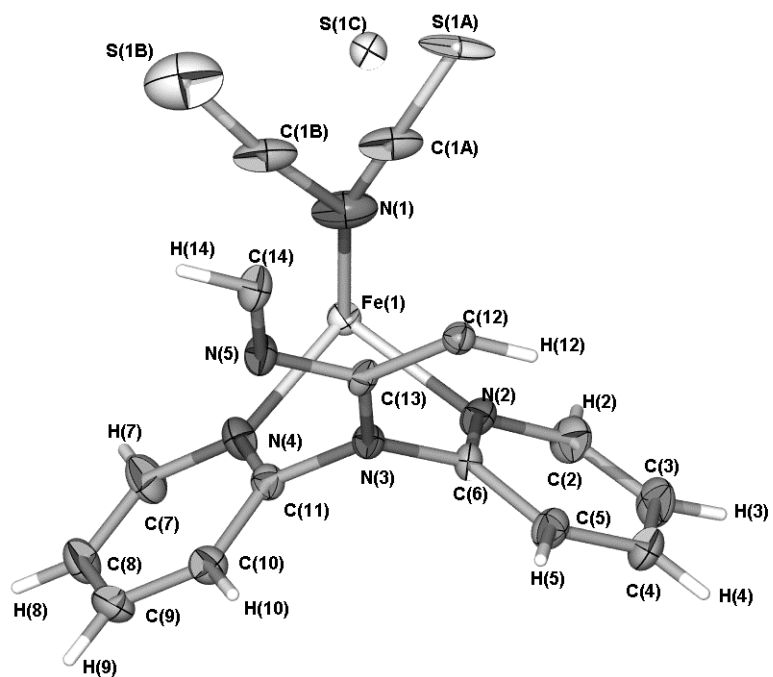


Figure S5. ORTEP representation (50 % probability) of the crystal structure of **2a** at 123 K highlighting the numbering scheme.

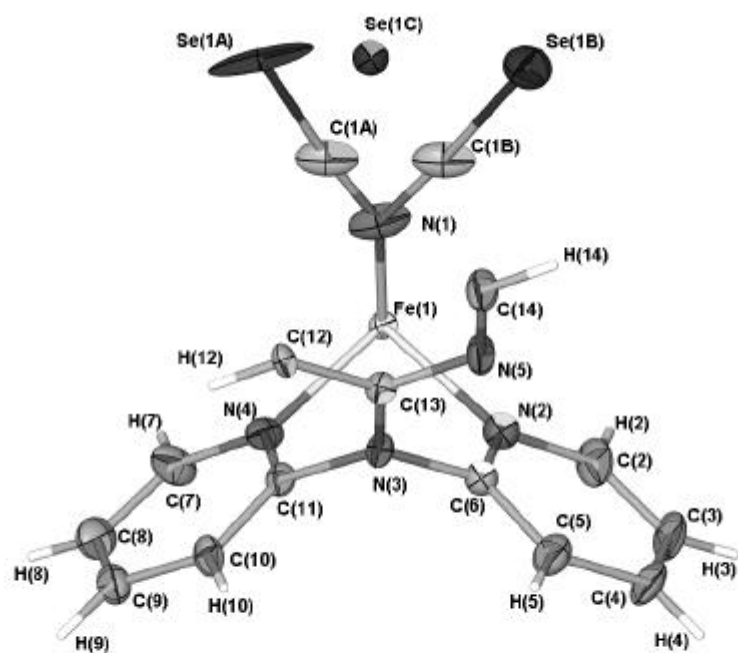


Figure S6. ORTEP representation (50 % probability) of the crystal structure of **2b** at 100 K highlighting the numbering scheme. The same scheme is used for **2b^{LS}**, **2b^{LS/HS}** and **2b^{HS}**